

# STRONGLY-ENTANGLED TWIN BEAMS PRODUCED BY A COHERENT BEAT LASER COUPLED TO THERMAL RESERVOIR

Chimdessa Gashu Feyisa,<sup>1\*</sup> Tamirat Abebe,<sup>1</sup> Teklemariam Tessema,<sup>1</sup>  
Ebisa Mosisa,<sup>1</sup> Abebe Tuguma,<sup>1</sup> Jiregna Amsalu,<sup>1</sup> Adimasu Worku,<sup>1</sup>  
Gemechu Feyisa,<sup>1</sup> Demissie Jobir,<sup>2</sup> and Mekonnen Molla<sup>3</sup>

<sup>1</sup>*Department of Physics, Jimma University  
P.O. Box 378, Jimma, Ethiopia*

<sup>2</sup>*Department of Electronics and Communicatios  
Adama Sciences and Technology  
P.O. Box 1888, Adama, Ethiopia*

<sup>3</sup>*Department of Physics, Aksum University  
P.O. Box 1010, Axum, Ethiopia*

\*Corresponding author e-mail: chimdessagashu@gmail.com

## Abstract

Applying the combination of the master and stochastic differential equations, we investigate in detail a continuous-variable entanglement of the twin beam generated by the coherent beat laser containing a parametric amplifier and coupled to thermal light of an external environment. The dipole-forbidden transition of the three-level atoms are coupled by the initial coherent superposition and classical pumping light emerging from the parametric oscillator. The atomic coherence induced by the classical pumping field and the initial coherent superposition induce a strong correlation between the two-mode radiation, which results in a high degree of the photon entanglement. In addition, the parametric amplifier enhances the achievable degree of entanglement of the two-mode fields. On the other hand, thermal light appears to degrade entanglement but a strong photon entanglement can be generated by managing the amount of thermal noise entering into the laser cavity through the output mirror.

**Keywords:** entanglement, injected atomic coherence, driven atomic coherence, thermal decoherence, inseparability criteria.

## 1. Introduction

Quantum entanglement is the nonclassical and nonlocal aspect of quantum correlations. It is the property attributed to pairs or groups of particles such as photons [1], electrons [2], atoms [3], etc. This wonderful nonclassical feature was first investigated in the EPR seminal paper by A. Einstein, B. Podolsky, and R. Rosen [4] and recognized as a nonclassical property of quantum correlations by S. Bell [5]. After the advent of quantum theory, entanglement has been utilized as a key resource for quantum computers [6], quantum information and communication [7], quantum dense coding [8], secure communication via quantum teleportation [9], and quantum sensing and metrology through atom clocks and interferometers [10]. Quantum entanglement is exhibited for highly-intense beam of light unlike the photon antibunching radiation fields.

Extensive research has shown that a three-level cascade laser could produce an entangled twin beams [11–22], when coupled by either coherent superposition [17, 18] or classical field [19–21] or using these mechanisms together [22]. On the other hand, the parametric amplifier, in addition to its role as a source of entanglement and other nonclassical features by itself [23, 24], can be introduced into other optical devices as means of amplifying the nonclassical features. In this line, some authors have also studied quantum properties of light generated by the three-level laser with a parametric amplifier and coupled to ordinary and squeezed-vacuum reservoirs [25–27]. These works have indicated that the parametric amplifier has a significant influence on the quantum features of radiation in the laser cavity. On the other hand, it is well known that the quantum features, including entanglement, are very sensitive to and easily degrade in a noisy external environments such as thermal reservoir, and the statistical features are perceptibly altered as well [28].

Therefore, the assumption that the laser cavity is coupled to a vacuum environment, which was commonly used so far, has neglects the role of an external noise on the quantum properties and photon statistics of a system. This assumption would never be satisfied unless we can completely isolate our laser cavity from an external environment, so that no excitations will be exchanged with a laser system. However, it is quite cumbersome for real physical situations to be free from the effect of an external environment, which is very natural and inevitably decouples the atomic correlations responsible for the quantum and statistical properties [29, 30]. On the other hand, the quantum and statistical features of radiation in the laser cavity increase with the parametric amplifier [31]. With this motivation, we devote our work to investigate influences of these competing physical processes on the nonclassical properties of radiation generated by a nondegenerate three-level cascade laser, whose cavity contains a nondegenerate parametric amplifier and is coupled to two-mode thermal reservoir.

In this study, we analyze the entanglement of a two-mode light produced by a nondegenerate three-level laser with a nondegenerate parametric amplifier and coupled to two-mode thermal reservoir. We also introduce the parametric amplifier, and both driven and injected atomic coherences, which can play competitive role with the thermal decoherence. In order to carry out our analysis, we first derive the master equation in the good cavity limit, linear and adiabatic approximations following the standard method developed in [23, 24, 28]. Applying the master equation, we obtain the stochastic-noise forces and solutions of the laser-cavity-mode operators arranged in the normal order. Applying the resulting solutions, we investigate the entanglement and intensity of light in the laser cavity.

## 2. The Model and Its Solution

We consider a nondegenerate three-level laser with a nondegenerate parametric amplifier (NDPA) coupled to a two-mode thermal source as shown in Fig. 1. The three-level atoms, which are initially prepared in a coherent superposition of the upper- and down-level states, are injected into the cavity at a constant rate and removed from the laser cavity after some time. We discuss the case where the laser cavity contains a nondegenerate parametric amplifier, and the laser-cavity modes are coupled to thermal reservoir; see Fig 1. The pump mode emerging from the parametric amplifier does not couple the upper and down levels of the three-level atoms. Instead, a classical driving radiation from another source is employed to couple the dipole-forbidden transition. As it is clearly indicated, the upper, middle, and down levels of a three-level atom are represented by  $|l\rangle$ ,  $|m\rangle$ , and  $|n\rangle$ , respectively.

We assume that transitions between levels  $|l\rangle$  and  $|m\rangle$  and between levels  $|m\rangle$  and  $|n\rangle$  are dipole allowed, with direct transition between levels  $|l\rangle$  and  $|n\rangle$  being dipole forbidden. This means that states

$|n\rangle$  and  $|l\rangle$  have the same parity. Therefore, the wave function describing the upper- and down-level states is either even or odd for both states. On the other hand, the middle state  $|m\rangle$  has the opposite parity, with its wave function being either odd or even but in contrast to that of the upper- and down-level states. The cavity radiation modes are at resonance with the transitions  $|l\rangle \rightarrow |m\rangle$  and  $|m\rangle \rightarrow |n\rangle$  having frequencies  $\omega_{lm}$  and  $\omega_{mn}$ , respectively. In the nondegenerate three-level laser, a pump mode of frequency  $\omega = \omega_{lm} + \omega_{mn}$  interacts with the nondegenerate parametric amplifier (NDPA) to produce the signal-idler photon pairs with the same frequencies as the two-dipole-allowed atomic transitions [23, 24, 28].

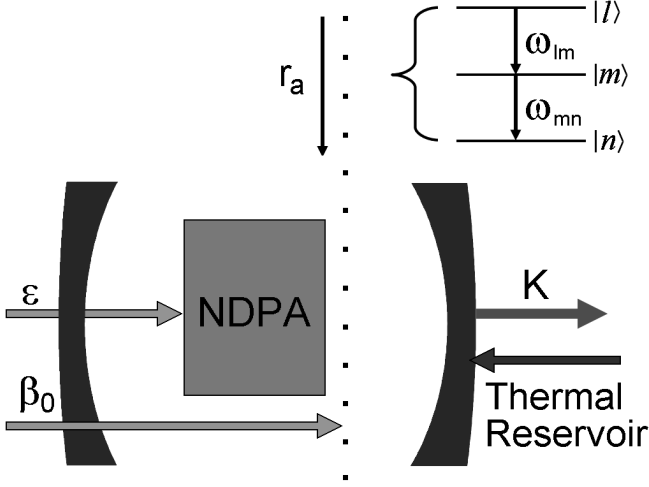


**Fig. 1.** Schematic representation of nondegenerate three-level laser with a nondegenerate parametric amplifier (NDPA) and coupled to a two-mode thermal reservoir.

A nondegenerate parametric amplifier, with the pump mode being treated classically and setting  $\hbar = 1$ , can be described by the interaction Hamiltonian in the interaction picture with the electric-dipole and rotating-wave approximations as follows [24]:

$$\hat{H}_{\text{NDPA}} = i\varepsilon(\hat{a}^\dagger\hat{b}^\dagger - \hat{a}\hat{b}), \quad (1)$$

where  $\varepsilon$  is a real constant proportional to the amplitude of the pump mode that drives the nonlinear crystal, and  $\hat{a}$  and  $\hat{b}$  are the annihilation operators for the two cavity modes.

On the other hand, the interaction of a three-level atom with the two-mode laser-cavity light can be expressed in the interaction picture with the rotating-wave and electric-dipole approximations by the quantum Hamiltonian for  $\hbar = 1$  as [23]

$$\hat{H}_{\text{RA}} = i\nu[\hat{a}^\dagger|m\rangle\langle l| + \hat{b}^\dagger|n\rangle\langle m| - \hat{a}|l\rangle\langle m| - \hat{b}|m\rangle\langle n|] + i\frac{\Omega}{2}[|n\rangle\langle l| - |l\rangle\langle n|], \quad (2)$$

where  $\nu$  is a real constant parameter of the interaction; it is considered to be the same for both transitions,  $\Omega = 2\mu\beta_0$ , in which  $\beta_0$  is the amplitude of the classical driving field and  $\mu$  is the coupling constant between the classical driving field and the three-level atom. The last term in this equation indicates the coupling of the upper and down levels by a classical pumping field.

Next, we consider the atoms initially prepared in a coherent superposition of the upper-level  $|l\rangle$  and down-level  $|n\rangle$  states, i.e.,

$$|\phi(0)\rangle = A_l|l\rangle + A_n|n\rangle, \quad (3)$$

where  $A_l = \langle l|\phi(0)\rangle$  and  $A_n = \langle n|\phi(0)\rangle$  are the probability amplitudes for the atom to be at the upper and down levels, respectively. The initial density operator for a single atom reads

$$\hat{\rho}_A(0) = \rho_l(0)|l\rangle\langle l| + \rho_n(0)|n\rangle\langle n| + \rho_{ln}(0)|l\rangle\langle n| + \rho_{nl}(0)|n\rangle\langle l|, \quad (4)$$

where  $\rho_l(0) = A_l A_l^*$  and  $\rho_n(0) = A_n A_n^*$  indicate the probability of the atoms to be at the upper and down levels, whereas  $\rho_{ln}(0) = \rho_{nl}^*(0) = A_l A_n^*$  represents the initial atomic coherence. The off-diagonal terms in Eq. (4) are zero in statistical mixture. On the other hand, in a coherent superposition of the upper- and down-level states of the three-level atom, these terms are not zero. These terms are accountable for

many interesting physical properties that could only be understood employing the quantum theory of light.

The three-level atoms, which are initially prepared in a coherent superposition of the excited and ground states, resonantly interact with the laser-cavity modes and external pumping radiation within the cavity mirrors. We apply the linear approximation, which preserves the quantum properties of the radiation in the optical system. After that, the atomic variables are adiabatically eliminated keeping the net effective laser-cavity-mode equation containing the remaining atomic variables in the good cavity limit. Now, we apply the linear and adiabatic approximation schemes and Eq. (2) to find the time evolution of the density operator for the laser-cavity mode; it reads

$$\begin{aligned} \frac{d\hat{\rho}}{dt} = & \frac{AI}{2\Upsilon}(2\hat{a}^\dagger\hat{\rho}\hat{a} - \hat{a}\hat{a}^\dagger\hat{\rho} - \hat{\rho}\hat{a}\hat{a}^\dagger) + \frac{AM}{2\Upsilon}(2\hat{b}\hat{\rho}\hat{b}^\dagger - \hat{b}^\dagger\hat{b}\hat{\rho} - \hat{\rho}\hat{b}^\dagger\hat{b}) \\ & + \frac{AN}{2\Upsilon}(\hat{a}^\dagger\hat{\rho}\hat{b}^\dagger - \hat{\rho}\hat{b}^\dagger\hat{a}^\dagger + \hat{b}\hat{\rho}\hat{a} - \hat{a}\hat{\rho}\hat{b}) + \frac{AL}{2\Upsilon}(\hat{a}^\dagger\hat{\rho}\hat{b}^\dagger - \hat{b}^\dagger\hat{a}^\dagger\hat{\rho} + \hat{b}\hat{\rho}\hat{a} - \hat{\rho}\hat{a}\hat{b}), \end{aligned} \quad (5)$$

where  $A = \frac{2\nu^2 r_a}{\gamma_s^2}$  is the linear gain coefficient, which can be defined as an effective rate of atomic injection; the rest parameters,  $\nu$  and  $\gamma_s$ , are constant parameters,

$$\Upsilon = (1 + \zeta^2)(4 + \zeta^2), \quad I = \rho_l(0)(4 + \zeta^2) + \rho_n(0)3\zeta^2 - \rho_{ln}(0)6\zeta, \quad (6)$$

and

$$\begin{aligned} M &= \rho_l(0)3\zeta^2 + \rho_n(0)(4 + \zeta^2) + \rho_{ln}(0)6\zeta, \\ N &= -\rho_l(0)\zeta(2 - \zeta^2) + \rho_n(0)\zeta(4 + \zeta^2) - \rho_{ln}(0)2(2 - \zeta^2), \\ L &= -\rho_l(0)\zeta(4 + \zeta^2) + \rho_n(0)\zeta(2 - \zeta^2) - \rho_{ln}(0)2(2 - \zeta^2), \end{aligned} \quad (7)$$

with  $\zeta = \Omega/\gamma$ ; we have set  $\rho_{ln}(0) = \rho_{nl}(0)$  to reduce the mathematical complexity.

In addition, the time evolution of the density operator for a two-mode cavity radiation coupled to a two-mode thermal reservoir via a single-port mirror is found to be [28]

$$\begin{aligned} \frac{d\hat{\rho}}{dt} = & -i[\hat{H}_{\text{NDPA}} + \hat{H}_{\text{RA}}, \hat{\rho}(t)] + \frac{\kappa}{2}\bar{n}_{\text{th}}(2\hat{a}^\dagger\hat{\rho}\hat{a} - \hat{a}\hat{a}^\dagger\hat{\rho} - \hat{\rho}\hat{a}\hat{a}^\dagger) + \frac{\kappa}{2}(\bar{n}_{\text{th}} + 1)(2\hat{a}\hat{\rho}\hat{a}^\dagger - \hat{a}^\dagger\hat{a}\hat{\rho} - \hat{\rho}\hat{a}^\dagger\hat{a}) \\ & + \frac{\kappa}{2}(\bar{n}_{\text{th}} + 1)(2\hat{b}\hat{\rho}\hat{b}^\dagger - \hat{b}^\dagger\hat{b}\hat{\rho} - \hat{\rho}\hat{b}^\dagger\hat{b}) + \frac{\kappa}{2}\bar{n}_{\text{th}}(2\hat{b}^\dagger\hat{\rho}\hat{b} - \hat{b}\hat{b}^\dagger\hat{\rho} - \hat{\rho}\hat{b}\hat{b}^\dagger), \end{aligned} \quad (8)$$

where  $\kappa_a = \kappa_b = \kappa$  are the cavity damping constant, and  $n_{\text{th}}$  is the mean photon number of thermal reservoir.

Now, with the help of Eqs. (1), (5), and (8), the evolution equation of the density operator for the cavity light is expressed as

$$\begin{aligned} \frac{d\hat{\rho}}{dt} = & \varepsilon[\hat{\rho}\hat{a}\hat{b} - \hat{a}\hat{b}\hat{\rho} + \hat{a}^\dagger\hat{b}^\dagger\hat{\rho} - \hat{\rho}\hat{a}^\dagger\hat{b}^\dagger] + \frac{\kappa}{2}(\bar{n}_{\text{th}} + 1)[2\hat{a}\hat{\rho}\hat{a}^\dagger - \hat{a}^\dagger\hat{a}\hat{\rho} - \hat{\rho}\hat{a}^\dagger\hat{a}] + \frac{1}{2}\kappa\bar{n}_{\text{th}}[2\hat{b}^\dagger\hat{\rho}\hat{b} - \hat{b}\hat{b}^\dagger\hat{\rho} - \hat{\rho}\hat{b}\hat{b}^\dagger] \\ & + \frac{1}{2}\left(\frac{AI}{\Upsilon} + \kappa\bar{n}_{\text{th}}\right)[2\hat{a}^\dagger\hat{\rho}\hat{a} - \hat{a}\hat{a}^\dagger\hat{\rho} - \hat{\rho}\hat{a}\hat{a}^\dagger] + \frac{1}{2}\left(\frac{AM}{\Upsilon} + \kappa(\bar{n}_{\text{th}} + 1)\right)[2\hat{b}\hat{\rho}\hat{b}^\dagger - \hat{b}^\dagger\hat{b}\hat{\rho} - \hat{\rho}\hat{b}^\dagger\hat{b}] \\ & - \frac{AN}{2\Upsilon}[\hat{a}\hat{b}\hat{\rho} - \hat{a}^\dagger\hat{\rho}\hat{b}^\dagger + \hat{\rho}\hat{b}^\dagger\hat{a}^\dagger - \hat{b}\hat{\rho}\hat{a}] - \frac{AL}{2\Upsilon}[\hat{b}^\dagger\hat{a}^\dagger\hat{\rho} - \hat{a}^\dagger\hat{\rho}\hat{b}^\dagger + \hat{\rho}\hat{a}\hat{b} - \hat{b}\hat{\rho}\hat{a}]. \end{aligned} \quad (9)$$

This is the master equation for a coherent beat laser, whose cavity contains a nondegenerate parametric amplifier and is coupled to a two-mode thermal reservoir. The quantum and statistical properties of the light generated by a coherent beat laser with a nondegenerate parametric amplifier and coupled to thermal reservoir are determined by this equation. The above master equation helps to derive the equations of motion for the expectation values of various system operators. The first term, which contains the cross-correlated operators, arises from the incorporation of the nonlinear crystal into the cavity. The terms proportional to  $I$  and  $M$  describe the gain of light in the laser cavity for mode  $\hat{a}$  and the loss for mode  $\hat{b}$ , respectively. The last two terms, which are proportional to  $N$  and  $L$ , are related to the correlation of the generated radiation that indicates the existence of quantum features. Furthermore, the terms proportional to  $\kappa$  describe the laser-cavity damping rate.

It is more suitable to introduce a new parameter  $x$  to relate the initial probabilities of the atoms initially populating at different energy levels. Hence, we denote  $x = \rho_n(0) - \rho_{n'}(0)$  and  $\rho_{tn}(0) = \frac{\sqrt{1-x^2}}{2}$  provided that  $-1 \leq x \leq 1$ . On the basis of Eq. (9), we can write

$$\frac{d}{dt}\alpha(t) = -c_+\alpha(t) - d_+\beta^*(t) + f_\alpha(t), \quad \frac{d}{dt}\beta^*(t) = -c_-\beta^*(t) - d_-\alpha(t) + f_\beta^*(t), \quad (10)$$

where

$$c_\pm = \frac{1}{2} \left\{ \kappa + \frac{A}{2\Upsilon} \left[ \frac{3\zeta}{2} \sqrt{1-x^2} + x \left( 1 - \frac{\zeta^2}{2} \right) \mp (1 + \zeta^2) \right] \right\}, \quad (11)$$

$$d_\pm = -\frac{1}{2} \left[ 2\varepsilon + \frac{A}{2\Upsilon} \left( \frac{\zeta}{2}(1 + \zeta^2) \pm \left\{ \frac{3x\zeta}{2} - \sqrt{1-x^2} \left( 1 - \frac{\zeta^2}{2} \right) \right\} \right) \right], \quad (12)$$

and  $f_\alpha(t)$  and  $f_\beta^*(t)$  are noise forces, the correlation properties of which are given by

$$\langle f_\alpha(t) \rangle = \langle f_\beta(t) \rangle = \langle f_\alpha(t')f_\alpha(t) \rangle = \langle f_\beta(t)f_\beta(t') \rangle = \langle f_\alpha^*(t)f_\beta(t') \rangle = 0, \quad (13)$$

$$\langle f_\alpha(t')f_\alpha^*(t) \rangle = [(AI/\Upsilon) + \kappa\bar{n}_{\text{th}}]\delta(t-t'), \quad \langle f_\beta(t')f_\beta^*(t) \rangle = \kappa\bar{n}_{\text{th}}\delta(t-t'), \quad (14)$$

$$\langle f_\beta(t')f_\alpha(t) \rangle = -[(AL - 2\varepsilon\Upsilon)/2\Upsilon]\delta(t-t'). \quad (15)$$

We note that Eqs. (13)–(15) represent the correlation properties of the noise forces associated with the normal ordering. These correlation functions are very useful to describe random processes. The coupled differential equations given in Eq. (10) can be described in a matrix form as

$$\frac{z(t)}{dt} = -mz(t) + \Delta(t), \quad (16)$$

where  $z(t) = \begin{pmatrix} \alpha^*(t) \\ \beta(t) \end{pmatrix}$ ,  $m = \begin{pmatrix} \xi_+^* & \eta_+^* \\ \eta_- & \xi_- \end{pmatrix}$ , and  $\Delta(t) = \begin{pmatrix} f_\alpha^*(t) \\ f_\beta(t) \end{pmatrix}$ .

After straightforward mathematical steps, we found the solutions of Eq. (16); they are

$$\alpha(t + \tau) = \frac{1}{2}[(1 + p)e^{-\lambda-\tau} + (1 - p)e^{-\lambda+\tau}]\alpha(t) + \frac{q_+}{2}[e^{-\lambda+\tau} - e^{-\lambda-\tau}]\beta^*(t) + \xi_+(t + \tau) + \varpi_+(t + \tau), \quad (17)$$

$$\beta(t + \tau) = \frac{1}{2}[(1 - p)e^{-\lambda-\tau} + (1 + p)e^{-\lambda+\tau}]\beta(t) + \frac{q_-}{2}[e^{-\lambda+\tau} - e^{-\lambda-\tau}]\alpha^*(t) + \xi_-(t + \tau) + \varpi_-(t + \tau), \quad (18)$$

where

$$\xi_+(t + \tau) = \frac{1}{2} \int_0^\tau \left[ (1+p)e^{-\lambda_-(\tau-\tau')} + (1-p)e^{-\lambda_+(\tau-\tau')} \right] f_\alpha(t + \tau') d\tau', \quad (19)$$

$$\xi_-(t + \tau) = \frac{1}{2} \int_0^\tau \left[ (1-p)e^{-\lambda_-(\tau-\tau')} + (1+p)e^{-\lambda_+(\tau-\tau')} \right] f_\beta(t + \tau') d\tau', \quad (20)$$

$$\varpi_+(t + \tau) = \frac{q_+}{2} \int_0^\tau \left[ e^{-\lambda_+(\tau-\tau')} - e^{-\lambda_-(\tau-\tau')} \right] f_\beta^*(t + \tau') d\tau', \quad (21)$$

$$\varpi_-(t + \tau) = \frac{q_-}{2} \int_0^\tau \left[ e^{-\lambda_+(\tau-\tau')} - e^{-\lambda_-(\tau-\tau')} \right] f_\alpha^*(t + \tau') d\tau', \quad (22)$$

with

$$p = \frac{1 + \zeta^2}{\sqrt{(1 + \zeta^2)^2 + \left[ (\zeta/2)(1 + \zeta^2) + 4\varepsilon\Upsilon/A \right]^2 - \left[ (3x\zeta/2) - \sqrt{1 - x^2}(1 - \zeta^2/2) \right]^2}}, \quad (23)$$

$$q_\pm = \frac{-\left[ (\zeta/2)(1 + \zeta^2) + 4\varepsilon\Upsilon/A \right] \mp \left[ (3x\zeta/2) - \sqrt{1 - x^2}(1 - \zeta^2/2) \right]}{\sqrt{(1 + \zeta^2)^2 + \left[ (\zeta/2)(1 + \zeta^2) + 4\varepsilon\Upsilon/A \right]^2 - \left[ (3x\zeta/2) - \sqrt{1 - x^2}(1 - \zeta^2/2) \right]^2}}, \quad (24)$$

$$\lambda_\pm = \frac{\kappa}{2} + \frac{A}{4\Upsilon} \left[ (3\zeta/2)\sqrt{1 - x^2} + x(1 - \zeta^2/2) \right] \pm \left[ (1 + \zeta^2)^2 + \left[ (\zeta/2)(1 + \zeta^2) + 4\varepsilon\Upsilon/A \right]^2 - \left[ (3x\zeta/2) - \sqrt{1 - x^2}(1 - \zeta^2/2) \right]^2 \right]^{1/2}. \quad (25)$$

We observe that the evolution equations for  $\alpha(t)$  and  $\beta(t)$  described in Eq. (10) do have well-behaved solutions iff the matrix  $m$  in Eq. (16) is negative, which is the condition for nondiverging solution. Based on this,  $\det(m) = 0$  or  $\lambda_\pm = 0$  is the threshold condition for the system [32]. Now we take the initial states of the laser-cavity modes to be the vacuum state, use the fact that the noise force at some time  $t$  does not affect the laser-cavity-mode variables at earlier times, and apply Eqs. (13)–(15), (17), and (18) to find the various expectation values of the laser-cavity-mode variables; they read

$$\langle \alpha^2 \rangle = \langle \beta^2 \rangle = \langle \alpha^* \beta \rangle = 0, \quad (26)$$

$$\begin{aligned} \langle \alpha^* \alpha \rangle &= \left( \frac{AI}{\Upsilon} + \kappa \bar{n}_{\text{th}} \right) \frac{\lambda_+^2 + \lambda_-^2 + 6\lambda_+ \lambda_-}{8\lambda_+ \lambda_- (\lambda_+ + \lambda_-)} + \left[ \left( \frac{AI}{\Upsilon} + \kappa \bar{n}_{\text{th}} \right) p^2 + \kappa \bar{n}_{\text{th}} q_+^2 + \left( \frac{AL}{\Upsilon} - 2\varepsilon \right) pq_+ \right] \\ &\times \frac{(\lambda_+ - \lambda_-)^2}{8\lambda_+ \lambda_- (\lambda_+ + \lambda_-)} + \left[ \left( \frac{AI}{\Upsilon} + \kappa \bar{n}_{\text{th}} \right) p + \left( \frac{AL}{2\Upsilon} - \varepsilon \right) q_+ \right] \frac{\lambda_+ - \lambda_-}{4\lambda_+ \lambda_-}, \end{aligned} \quad (27)$$

$$\begin{aligned} \langle \beta^* \beta \rangle &= \kappa \bar{n}_{\text{th}} \frac{\lambda_+^2 + \lambda_-^2 + 6\lambda_+ \lambda_-}{8\lambda_+ \lambda_- (\lambda_+ + \lambda_-)} + \left[ \left( \frac{AI}{\Upsilon} + \kappa \bar{n}_{\text{th}} \right) q_-^2 + \kappa \bar{n}_{\text{th}} p^2 - \left( \frac{AL}{\Upsilon} - 2\varepsilon \right) pq_- \right] \\ &\times \frac{(\lambda_+ - \lambda_-)^2}{8\lambda_+ \lambda_- (\lambda_+ + \lambda_-)} - \left[ \kappa \bar{n}_{\text{th}} p - \left( \frac{AL}{2\Upsilon} - \varepsilon \right) q_- \right] \frac{\lambda_+ - \lambda_-}{4\lambda_+ \lambda_-}, \end{aligned} \quad (28)$$

$$\begin{aligned} \langle \alpha \beta \rangle &= - \left( \frac{AL}{2\Upsilon} - \varepsilon \right) \frac{\lambda_+^2 + \lambda_-^2 + 6\lambda_+ \lambda_-}{8\lambda_+ \lambda_- (\lambda_+ + \lambda_-)} - \left[ \frac{AI}{\Upsilon} pq_- + \kappa \bar{n}_{\text{th}} p(q_+ - q_-) - \left( \frac{AL}{2\Upsilon} - \varepsilon \right) [p^2 - q_- q_+] \right] \\ &\times \frac{(\lambda_+ - \lambda_-)^2}{8\lambda_+ \lambda_- (\lambda_+ + \lambda_-)} - \left[ \left( \frac{AI}{\Upsilon} + \kappa \bar{n}_{\text{th}} \right) q_- + \bar{n}_{\text{th}} q_+ \right] \frac{\lambda_+ - \lambda_-}{4\lambda_+ \lambda_-}. \end{aligned} \quad (29)$$

### 3. Entanglement of the Two-Mode Radiation

In this section, we study the entanglement of the two-mode radiation in the laser cavity, in view of various inseparability criteria. A pair or group of particles are entangled if their states cannot be expressed as the product of the states of their separate constituents. The preparation and manipulation of these entangled states lead to a better understanding of the basic quantum principles [23, 28, 29]. Nowadays, a lot of criteria have been developed to measure, detect, and manipulate the entanglement generated by various quantum optical devices. Here, we consider the Duan–Giedke–Cirac–Zoller (DGCZ) criterion, the logarithmic negativity, the Hillery–Zubairy criterion, and the violation of the Cauchy–Schwarz inequality.

#### 3.1. Duan–Giedke–Cirac–Zoller (DGCZ) Criterion

First, we consider the entanglement criterion set by Duan et al. [33]. Based on this criterion, a quantum state of the system is entangled if the sum of the variances of the EPR-type operators  $\hat{u}$  and  $\hat{v}$  satisfies the condition  $\frac{\Delta u^2 + \Delta v^2}{2} < 1$ , in which

$$\hat{u} = \hat{x}_a - \hat{x}_b, \quad \hat{v} = \hat{p}_a + \hat{p}_b. \quad (30)$$

Here,  $\hat{x}_a = \frac{1}{\sqrt{2}}(\hat{a}^\dagger + \hat{a})$ ,  $\hat{x}_b = \frac{1}{\sqrt{2}}(\hat{b}^\dagger + \hat{b})$ ,  $\hat{p}_a = \frac{i}{\sqrt{2}}(\hat{a}^\dagger - \hat{a})$ , and  $\hat{p}_b = \frac{i}{\sqrt{2}}(\hat{b}^\dagger - \hat{b})$  are the quadrature operators of the cavity mode  $\hat{a}$  and  $\hat{b}$ . It is not difficult to find the sum of the variances of  $\hat{u}$  and  $\hat{v}$ ; it is

$$\frac{\Delta u^2 + \Delta v^2}{2} = 1 + \langle \alpha^* \alpha \rangle + \langle \beta^* \beta \rangle - 2\langle \alpha \beta \rangle; \quad (31)$$

this result represents the sum of fluctuations of the EPR-type quadrature operators of the two-mode radiation for a nondegenerate three-level cascade laser, whose cavity contains a nondegenerate parametric amplifier and is coupled to a two-mode thermal reservoir.

In order to investigate the entanglement dependence on the amplitude of the classical field, the initial preparation of the atoms, the amplitude of the parametric amplifier, and the linear gain coefficient, we plot Eq. (31) versus these parameters keeping some of them fixed; see Figs. 1 and 2. We found that the requirement of the uncertainty relation,  $\lambda_{\pm} \geq 0$ , holds for  $\bar{n}_{\text{th}} \geq 0$ ,  $0 \leq \varepsilon \leq 0.15$ ,  $A \leq 0.5$ ,  $\kappa = 0.5$ ,  $0 \leq x \leq 1$ , and  $\zeta \geq 0$ . The purpose of choosing the above numerical data is to investigate the nonclassical features of the radiation in the cavity for all values of the classical field. In addition, it is verified that the system under consideration properly operates for  $\bar{n}_{\text{th}} \geq 0$ ,  $0 \leq \varepsilon \leq 0.25$ ,  $A \geq 0$ ,  $\kappa = 0.5$ ,  $0 \leq x \leq 1$ , and  $\zeta \leq 0.002$ . Under these conditions, the system operates in the weak pumping regime. These numerical values are compatible with the parameters used in the micromaser experiments.

The entanglement dependence on the thermal noise for all amplitudes of the pump mode  $\varepsilon$  is presented in Fig. 2 a; here, the rate of atomic injections is limited to small value, so that the dependence of the entanglement in the weak and strong driving regimes can be observed. We see that the entanglement is highly suppressed by thermal noise from the environment outside the cavity. This indicates that higher degree of entanglement prefers a vacuum environment with zero mean photon number. There is no limitation on the value of  $\bar{n}_{\text{th}}$  imposed by the steady-state condition although its further manipulation completely destroys the entanglement. Also we observe that the entanglement can increase with the amplitude of the classical driving radiation in both regimes until its maximum degree is attained. However,

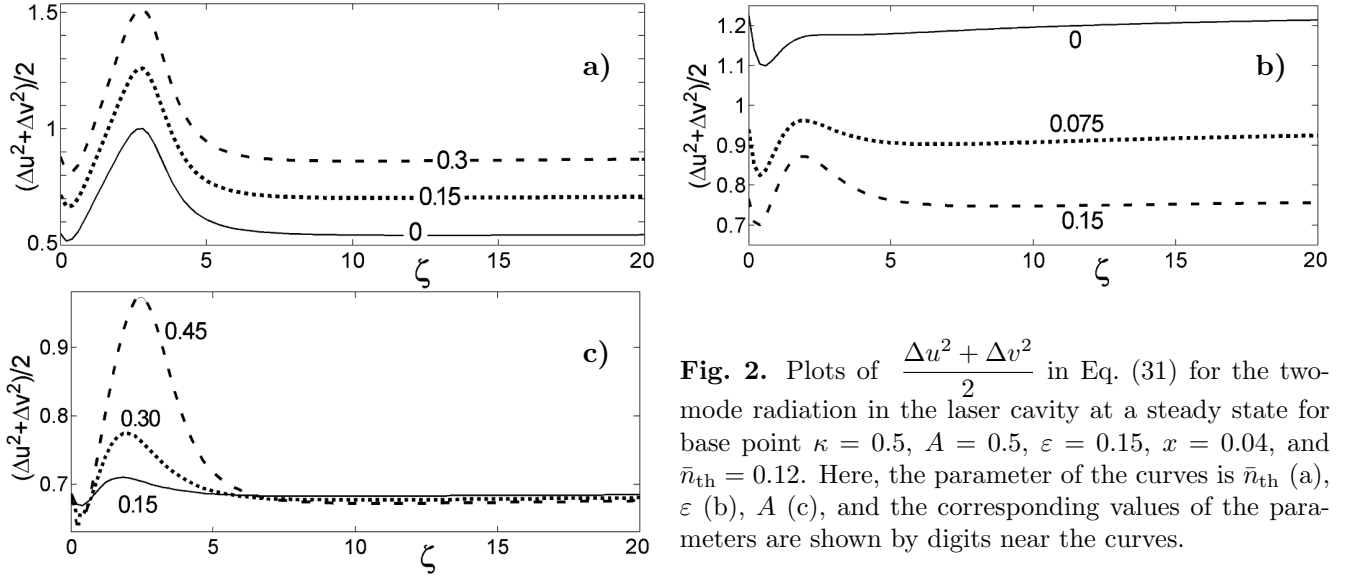


**Fig. 2.** Plots of  $\frac{\Delta u^2 + \Delta v^2}{2}$  in Eq. (31) for the two-mode radiation in the laser cavity at a steady state for base point  $\kappa = 0.5$ ,  $A = 0.5$ ,  $\varepsilon = 0.15$ ,  $x = 0.04$ , and  $\bar{n}_{\text{th}} = 0.12$ . Here, the parameter of the curves is  $\bar{n}_{\text{th}}$  (a),  $\varepsilon$  (b),  $A$  (c), and the corresponding values of the parameters are shown by digits near the curves.

we verify that more than the required value of the amplitude of the classical driving radiation damps the amount of entanglement.

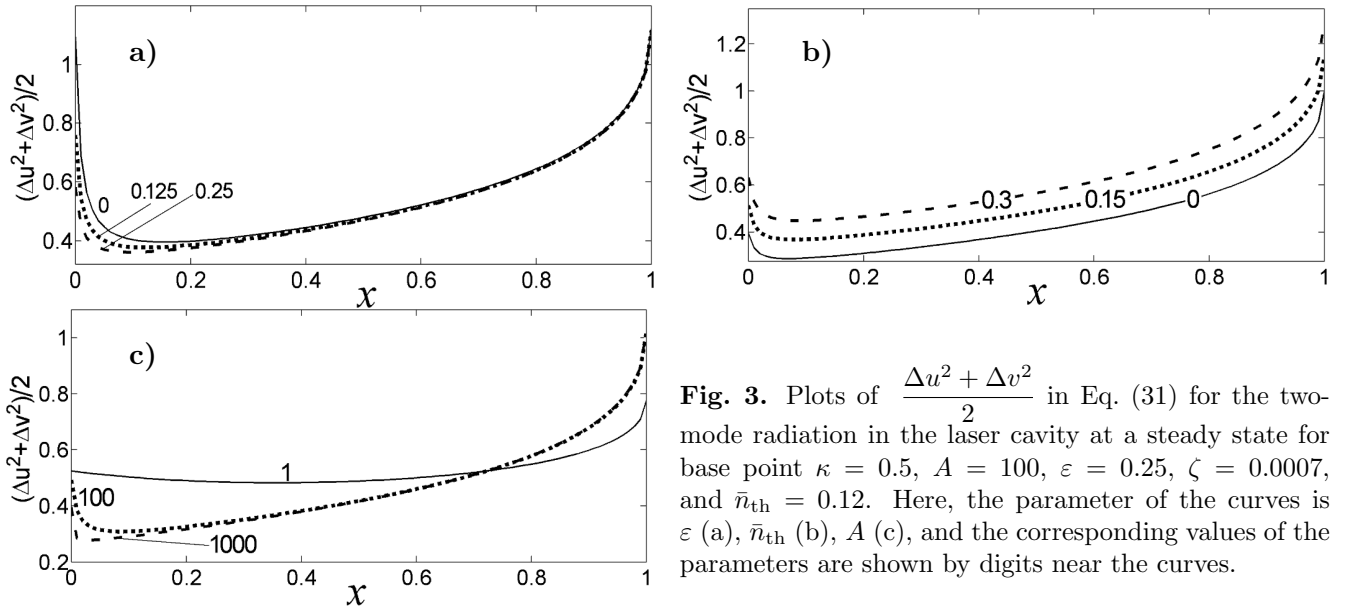
On the other hand, Fig. 2 b demonstrates that the parametric amplifier, in contrast to thermal noise, amplifies the entanglement of the radiation. One can clearly see that, in the absence of the parametric amplifier, the intra-cavity entanglement is also absent. However, the introduction of the parametric amplifier significantly amplifies the strength of entanglement. Unfortunately, the values of  $\varepsilon$  is limited due to the fact that it cannot be chosen arbitrarily.

Figure 2 c explicitly presents the possibility of generating a strong intra-cavity entangled light by manipulating the linear gain coefficient in the weak and strong driving regimes. Therefore, injecting more atoms into the laser cavity at a time improves the degree of entanglement.

The results presented in Fig. 2 make vivid that it is possible to produce a strong entangled light in the laser cavity by manipulating the various variables of the system under consideration, while the stronger entanglement occurs in the weak driving regime. In this regard, we seek to consider various specific cases to investigate the dependence of the entanglement of the intra-cavity radiation on the various quantities of interest in the weak driving regime.

It is clearly shown in Fig. 3 a that the two-mode radiation in the laser cavity exhibits entanglement for all values of the injected atomic coherence considered, except at the two limiting cases. We realize that for a system coupled to thermal environment of the mean photon number equal to 0.12, the introduction of a nonlinear crystal significantly improves the amount of the intra-cavity entanglement provided that sufficient atoms are initially prepared in the upper level (50%). This is related to the fact that larger value of  $\varepsilon$  corresponds to higher efficient down-conversion process. Unfortunately, we observed that this effect does not lead to entanglement at  $x = 1$ . Therefore, the parametric amplifier comes into play mostly when atoms are equally prepared in the down and upper levels ( $x \simeq 0$ ). In addition, we present the reduction of noise in EPR-quadrature variances in Table 1 for the plot shown in Fig. 3 a.





**Fig. 3.** Plots of  $\frac{\Delta u^2 + \Delta v^2}{2}$  in Eq. (31) for the two-mode radiation in the laser cavity at a steady state for base point  $\kappa = 0.5$ ,  $A = 100$ ,  $\varepsilon = 0.25$ ,  $\zeta = 0.0007$ , and  $\bar{n}_{\text{th}} = 0.12$ . Here, the parameter of the curves is  $\varepsilon$  (a),  $\bar{n}_{\text{th}}$  (b),  $A$  (c), and the corresponding values of the parameters are shown by digits near the curves.

**Table 1.** Numerical Value of the Sum of Noise in EPR-Type Quadrature Operators of the Laser-Cavity Radiation; Fig. 3 a.

$\varepsilon$	$(\Delta u^2 + \Delta v^2)/2$	Occurs at
0.00	0.395	$x = 0.162$
0.125	0.377	$x = 0.121$
0.25	0.361	$x = 0.091$

**Table 2.** Numerical Value of the Degree of Entanglement; Fig. 3 b.

$\bar{n}_{\text{th}}$	Degree of entanglement, %	Occurs at
0.00	72	$x = 0.071$
0.15	63.3	$x = 0.081$
0.30	55.3	$x = 0.091$

We immediately see from Fig. 3 b that the entanglement property of radiation in the laser cavity is significantly degraded by thermal noise even if a sufficiently large value of  $A$  is used. This nonclassical feature declines regardless of how atoms are initially prepared. Therefore, we notice that the entanglement is very sensitive nonclassical property of light that can be lost by a small effect of an external environment. Even then, it can be realized that a considerable amount of entanglement can be demonstrated by controlling the amount of thermal noise entering the laser cavity via its mirror. Numerical value of the degree of entanglement is presented in Table 2.

We clearly see in Fig. 3 c that the entanglement of light in the laser cavity increases with the linear gain coefficient for smaller values of  $x$ , but decreases for larger values of  $x$ . Thus, a substantial degree of entanglement is found for smaller values of  $x$ . This indicates that the degree of entanglement is highly related to the number of atoms injected into the cavity at a constant rate and the initial condition of the atoms before injection. When larger number of atoms, initially prepared in the excited state, are injected into the laser cavity, they absorb either radiation of the cavity modes thereby transferring

**Table 3.** Numerical Value of the Degree of Entanglement; Fig. 3 c.

$A$	Degree of entanglement, %	Occurs at
1	52	$x = 0.360$
100	70	$x = 0.091$
1000	73	$x = 0.030$

their coherence to the emitted photons. The transferred coherence among the emitted photons in turn generates the intra-cavity entanglement. It is worth noting that there is still a limitation on the value of  $A$  by the condition  $\Delta c_- \Delta c_+ \geq 1$  as we are confined to the weak driving regime. Such restriction on the rate of atomic injection does not exist in the strong driving regime, even if the amplification in this case is insignificant. We also observed that further increasing the linear gain coefficient, in which  $\lambda_{\pm} \geq 0$ , does not lead to a substantial degree of entanglement. Particularly, the degree of entanglement is illustrated in Table 3.

### 3.2. Logarithmic Negativity (LG) Criterion

The other widely-used entanglement measure is the logarithmic negativity, which is used for a two-mode continuous variables based on the negativity of the partial transposition [34, 35]. The logarithmic negativity for a two-mode light in the laser cavity is defined as  $E_N = \max[0, -\log_2 V_S]$ , in which  $V_S$  represents the smallest eigenvalue of the covariance matrix. According to this criterion, the entanglement is achieved when  $E_N$  is positive within the region of the smallest eigenvalue of the covariance matrix  $V_S < 1$  [35].

On the other hand, the eigenvalue of the covariance matrix is defined as

$$V_S = \left( \frac{\sigma - (\sigma^2 - 4 \det(G))^{1/2}}{2} \right)^{1/2}, \quad (32)$$

where the invariant matrix  $\sigma$  and covariance matrix  $G$  are [31, 36]

$$\sigma = \det(A_1) + \det(A_2) - 2 \det(A_{12}), \quad (33)$$

$$G = \begin{pmatrix} A_1 & A_{12} \\ A_{12}^T & A_2 \end{pmatrix}. \quad (34)$$

Here,  $A_1$  and  $A_2$  are the covariance matrices describing each mode separately, while  $A_{12}$  is the inter-mode correlation that leads to the observed nonclassical features detected by this criterion. The elements of the matrix in Eq. (34) are given by [34, 35]  $G_{ij} = \frac{1}{2}[\langle \hat{X}_i \hat{X}_j \rangle + \langle \hat{X}_j \hat{X}_i \rangle] - \langle \hat{X}_i \rangle \langle \hat{X}_j \rangle$ ;  $i, j = 1, 2, 3, 4$ , with  $\hat{X}_1 = \hat{a} + \hat{a}^\dagger$ ,  $\hat{X}_2 = i(\hat{a}^\dagger - \hat{a})$ ,  $\hat{X}_3 = \hat{b} + \hat{b}^\dagger$ , and  $\hat{X}_4 = i(\hat{b}^\dagger - \hat{b})$  being the quadrature operators corresponding to each light mode in the laser cavity.

The extended covariance matrix can be expressed in terms of the  $c$ -number variables associated with the normal ordering, in view of  $\langle \alpha\beta \rangle = \langle \alpha^* \beta^* \rangle$ , as follows:

$$G = \begin{pmatrix} 2\bar{n}_\alpha + 1 & 0 & 2\bar{n}_{\alpha\beta} & 0 \\ 0 & 2\bar{n}_\alpha + 1 & 0 & -2\bar{n}_{\alpha\beta} \\ 2\bar{n}_{\alpha\beta} & 0 & 2\bar{n}_\beta + 1 & 0 \\ 0 & -2\bar{n}_{\alpha\beta} & 0 & 2\bar{n}_\beta + 1 \end{pmatrix}, \quad (35)$$

where  $\bar{n}_\alpha = \langle \alpha^* \alpha \rangle$ ,  $\bar{n}_\beta = \langle \beta^* \beta \rangle$ , and  $\bar{n}_{\alpha\beta} = \langle \alpha\beta \rangle$ . Thus, on account of Eqs. (34) and (35), one can readily show that

$$\det A_1 = (2\bar{n}_\alpha + 1)^2, \quad \det A_2 = (2\bar{n}_\beta + 1)^2, \quad \det A_{12} = \det A_{12}^T = -4\bar{n}_{\alpha\beta}^2. \quad (36)$$

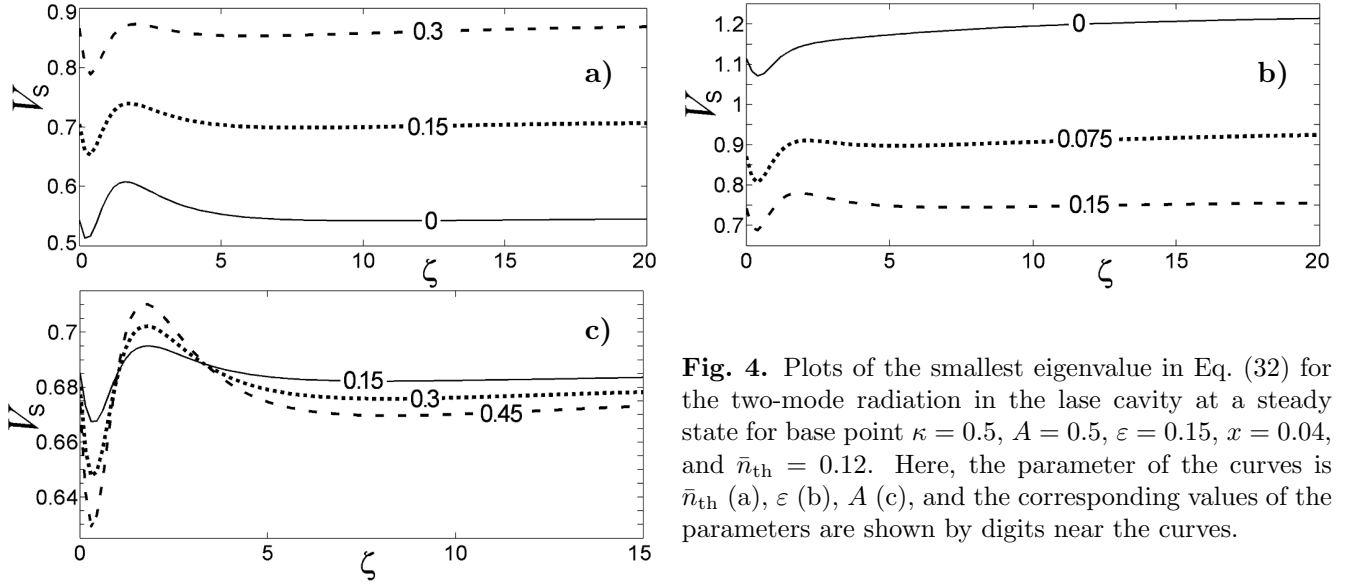


**Fig. 4.** Plots of the smallest eigenvalue in Eq. (32) for the two-mode radiation in the laser cavity at a steady state for base point  $\kappa = 0.5$ ,  $A = 0.5$ ,  $\varepsilon = 0.15$ ,  $x = 0.04$ , and  $\bar{n}_{th} = 0.12$ . Here, the parameter of the curves is  $\bar{n}_{th}$  (a),  $\varepsilon$  (b),  $A$  (c), and the corresponding values of the parameters are shown by digits near the curves.

It is also possible to establish that

$$\det G = [4(\bar{n}_\alpha \bar{n}_\beta - \bar{n}_{\alpha\beta}^2) + 2(\bar{n}_\alpha + \bar{n}_\beta) + 1]^2. \quad (37)$$

The result presented in Eq. (32), along with Eqs. (36) and (37), represents the steady-state expression of the smallest eigenvalue of the covariance matrix  $V_S$  for the quantum optical system.

In order to investigate the entanglement of the two-mode radiation with this criterion, we show the  $V_S$  dependence on the amplitude of the driving radiation, the initial preparation of the atoms, the amplitude of the parametric amplifier, and the linear gain coefficient for the same parameters as we used in the previous sections.

The dependence of the smallest eigenvalue of the covariance matrix on the mean photon number of the thermal environment and the amplitude of the classical driving radiation is presented in Fig. 4 a. The entanglement criterion,  $V_S < 1$  [35], is satisfied for all parameters under consideration. Also the value of  $V_S$  increases with increase in the thermal noise showing that the degree of entanglement is decreasing with increase in the mean photon number of the thermal noise. This is due to the fact that the thermal noise declines the atomic coherence that induces the nonclassical feature. Therefore, we can argue that the entanglement property of radiation in the laser cavity is very sensitive to the thermal environment and it can completely be lost when the thermal noise exceeds 0.51 ( $\bar{n}_{th} \geq 0.51$ ).

In contrast to the influence of the thermal reservoir,  $V_S$  decreases (the entanglement grows) with increase in the amplitude of the parametric amplifier in Fig. 4 b and the linear gain coefficient in Fig. 4 c. It is an encouraging result to see that the parametric amplifier and the linear gain coefficient play a competitive role with thermal reservoir in enhancing the degree of entanglement. It is clearly evident from Fig. 4 b that the parameter  $\varepsilon$  leads to entanglement, which is completely absent without the parametric amplifier; for instance, for  $\varepsilon = 0$ ,  $V_S > 1$  showing that the light is not entangled altogether. However, the introduction of the parametric amplifier leads to a considerable amount of entanglement.

On the other hand, the linear gain coefficient enhances the degree of entanglement before and after the threshold condition is attained; see Fig. 4 c. However, at the threshold, the degree of entanglement

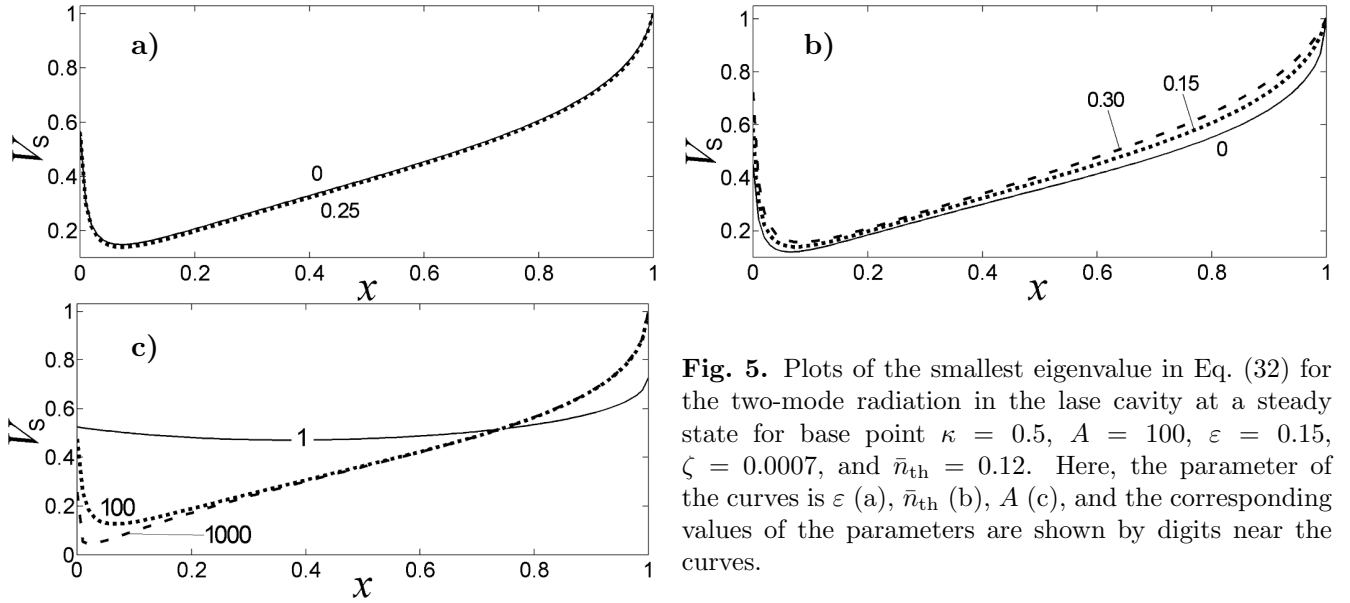


**Fig. 5.** Plots of the smallest eigenvalue in Eq. (32) for the two-mode radiation in the laser cavity at a steady state for base point  $\kappa = 0.5$ ,  $A = 100$ ,  $\varepsilon = 0.15$ ,  $\zeta = 0.0007$ , and  $\bar{n}_{\text{th}} = 0.12$ . Here, the parameter of the curves is  $\varepsilon$  (a),  $\bar{n}_{\text{th}}$  (b),  $A$  (c), and the corresponding values of the parameters are shown by digits near the curves.

decreases with the linear gain coefficient. This must be due to the spontaneous decay of atoms, which are initially prepared with the probability of 48% in the upper level, to levels that destroy the correlation among them at the threshold. It is worth noting that such phenomena is not observed in the absence of the external driving radiation.

Next, we investigate the smallest eigenvalue of the symplectic matrix in the weak driving regime to demonstrate the entanglement predicted by this criterion for the same parameters used in the analysis of the DGCZ criterion.

It is shown in Fig. 5 a that the light in the laser cavity is entangled except in the absence of the initial atomic coherence, and the entanglement strongly depends on the ways in which the atoms are initially prepared. Thus, the entanglement increases with the injected atomic coherence particularly for  $x \leq 0.0707$ , but decreases otherwise. The parametric amplifier is also somewhat enhances the degree of entanglement, but not significantly. In addition, we observe that the criterion predicts a robust entanglement of 87.2% for  $x = 0.0707$  and  $\varepsilon = 0.25$ , where the DGCZ criterion, with the same parameters, predicts 64% as shown in Fig. 5 a.

On the other hand, we learn that  $V_S \leq 1$  for all chosen parameters; see Fig. 5 b. The equality holds in the absence of the initial atomic coherence for which the entanglement is disappeared. The thermal noise increases  $V_S$  indicating that the entanglement property of light in the laser cavity suppresses with increase in the mean photon number of the thermal reservoir. However, the mean photon number of the thermal reservoir does not produce a significant variation in the degree of entanglement compared with the DGCZ criterion, as shown in Fig. 2 a. In addition, for the atoms initially prepared at  $x = 1$ , we observed that  $V_S = 1$ , no matter how we increase the mean photon number of thermal reservoir,  $\bar{n}_{\text{th}}$ . It is worth noting that stronger entangled light can be generated even when the laser cavity is coupled to a thermal environment of considerable mean photon number. Particularly, the degree of entanglement resulting from this criterion is presented in Table 4.

**Table 4.** Numerical Value of the Degree of Entanglement; Fig. 5 b.

$\bar{n}_{\text{th}}$	Degree of entanglement, %	Occurs at
0.00	88.8	$x = 0.0606$
0.15	86.6	$x = 0.0707$
0.30	84.4	$x = 0.0808$

**Table 5.** Comparison of the Amount of Entanglement Quantified by the Logarithmic Negativity and DGCZ Criteria.

$A$	DGCZ		LG	
	%	Occurs at	%	Occurs at
1	52	$x = 0.366$	53	$x = 0.366$
100	70	$x = 0.0909$	88.4	$x = 0.0707$
1000	73	$x = 0.0303$	95.7	$x = 0.0202$

Furthermore, we present in Fig. 5 c the possibility of producing a robust entangled light in the laser cavity by manipulating the linear gain coefficient with a proper choice of the initial atomic coherence. In addition, comparison of Figs. 5 c and 2 c shows that the logarithmic negativity criterion predicts a robust entangled light than the actually achievable degree of entanglement quantified by the DGCZ criterion. Also the degree of entanglement increases with the rate at which atoms are injected into the cavity, and it is found to be stronger for 48% of atoms initially populating in the upper level. The degree of entanglement quantified by the DGCZ criterion grows from 52% to 73% for the linear gain coefficient changes from  $A = 1$  to  $A = 1000$ . In this situation, the degree of entanglement varies from 53% to 95.7% by the LG criterion. Particularly, comparison of Figs. 2 c and 5 c gives the degree of entanglement quantified by the DGCZ and logarithmic negativity criteria as shown in Table 5.

### 3.3. Hillary–Zubairy (HZ) Criterion

According to the criterion introduced by Hillary and Zubairy, for two modes of the electromagnetic field with annihilation operators  $\hat{a}$  and  $\hat{b}$ , the composite state is said to be entangled, if the condition  $\langle \hat{a}\hat{b} \rangle > \sqrt{\langle \hat{a}^\dagger\hat{a} \rangle \langle \hat{b}^\dagger\hat{b} \rangle}$  is satisfied [34,37]. In this relation,  $\hat{n}_a$  and  $\hat{n}_b$  are the pertinent photon numbers corresponding to the involved modes, whereas  $\langle \hat{a}\hat{b} \rangle$  is the correlated mean photon number of the two-mode light. The criterion can be written in a more convenient form, namely,

$$F = \langle \hat{a}^\dagger\hat{a} \rangle \langle \hat{b}^\dagger\hat{b} \rangle - \langle \hat{a}\hat{b} \rangle^2, \quad (38)$$

where the negativity of the parameter  $F$  is a clear indication of the existence of entanglement [34,37]. In terms of the  $c$ -number, the steady state expression of Eq. (38) reads

$$F = \bar{n}_\alpha \bar{n}_\beta - \bar{n}_{\alpha\beta}^2. \quad (39)$$

In order to investigate the entanglement of light in the laser cavity with this criterion, we plot  $F$  versus  $\zeta$ ,  $\kappa$ ,  $\varepsilon$ ,  $A$ , and  $x$ , keeping some of them similar to the values used in the previous sections. This is useful to compare this criterion with the other entanglement criteria.

We immediately observe in Fig. 6 a that the parameter  $F$  is nonnegative for  $\varepsilon = 0$ , for which the condition in Eq. (39) fails and the light in the laser cavity is thus not entangled. On the other hand, the criterion holds for  $\varepsilon \neq 0$ ; in addition, we observe that as  $\varepsilon$  increases,  $F$  becomes more negative indicating the role of the parametric amplifier in enhancing the degree of entanglement similar to the DGCZ and logarithmic negativity criteria.

In the continuation, we present in Fig. 6 b the dependence of  $F$  on the amplitude of the classical driving radiation and the linear gain coefficient. In this case,  $F$  is negative for all parameters considered

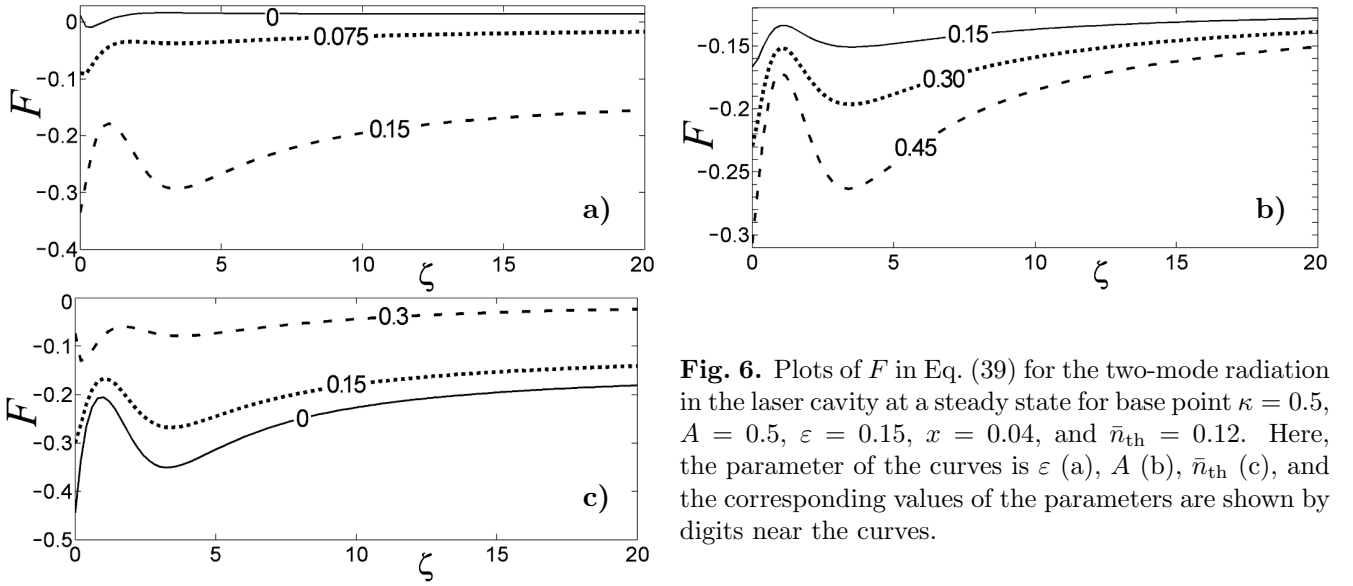


**Fig. 6.** Plots of  $F$  in Eq. (39) for the two-mode radiation in the laser cavity at a steady state for base point  $\kappa = 0.5$ ,  $A = 0.5$ ,  $\varepsilon = 0.15$ ,  $x = 0.04$ , and  $\bar{n}_{\text{th}} = 0.12$ . Here, the parameter of the curves is  $\varepsilon$  (a),  $A$  (b),  $\bar{n}_{\text{th}}$  (c), and the corresponding values of the parameters are shown by digits near the curves.

and becomes more negative with increase in the linear gain coefficient. The comparison of this result with Figs. 5 a and 2 c indicates that, as the negativity of  $F$  increases, the degree of entanglement also increases. This criterion demonstrates the same pattern of entanglement with the logarithmic negativity and DGCZ criteria, except for  $\zeta = 0$ .

In Fig. 6 c, we show that  $F$  is more negative by decreasing the mean photon number of the thermal reservoir. This result is also consistent with the previous criteria as the degree of entanglement declines with the mean photon number of the thermal reservoir.

We see in Fig. 6 that the parameter  $F$  is more negative in the weak driving regime than in the strong driving one. Therefore, we focus in the weak driving regime, where an improved strength of the entanglement is observed. To this effect, we consider various specific cases to investigate the dependence of  $F$  on the parametric amplifier, the linear gain coefficient, the mean photon number of thermal reservoir, and the initial preparation of the atoms in the weak driving regime.

In Fig. 7 a and b, we show the dependence of  $F$  on the linear gain coefficient, the amplitude of the parametric amplifier, and ways in which the atoms are initially prepared. Here,  $F$  is negative in both Fig. 7 a and b, except for  $x = 1$ . Also the influences of  $\varepsilon$  and  $A$  on  $F$  are more prominent for  $x \leq 0.2$ , at which the negativity of  $F$  grows rapidly, and the logarithmic negativity and DGCZ criteria predict the maximum degree of entanglement. Hence the HZ criterion demonstrates the entanglement property of the cavity radiation similar to the logarithmic negativity and DGCZ criteria. However, an issue that may arise regarding the HZ criterion is that there is no lower limit on the value of the parameter  $F$ . As a result, we could not exactly know the amount of entangled light defined, in view of this criterion, but we can clearly identify the stronger and weaker one separately.

In Fig. 7 c, we immediately see that the negativity of  $F$  increases with the mean photon number of the thermal environment particularly for  $x \geq 0.04$  and decreases otherwise. Entanglement disappears altogether in the absence of the initial atomic coherence ( $x \simeq 1$ ) since  $F$  is nonnegative. Comparison of Fig. 7 indicates that the HZ criterion does not exhibit substantial variation of entanglement for  $x \geq 0.2$ , unlike the other criteria. The HZ criterion also indicates a strong degree of entanglement (where  $F$  is more negative) for  $x = 0$ , which corresponds to the maximum injected atomic coherence and preparation

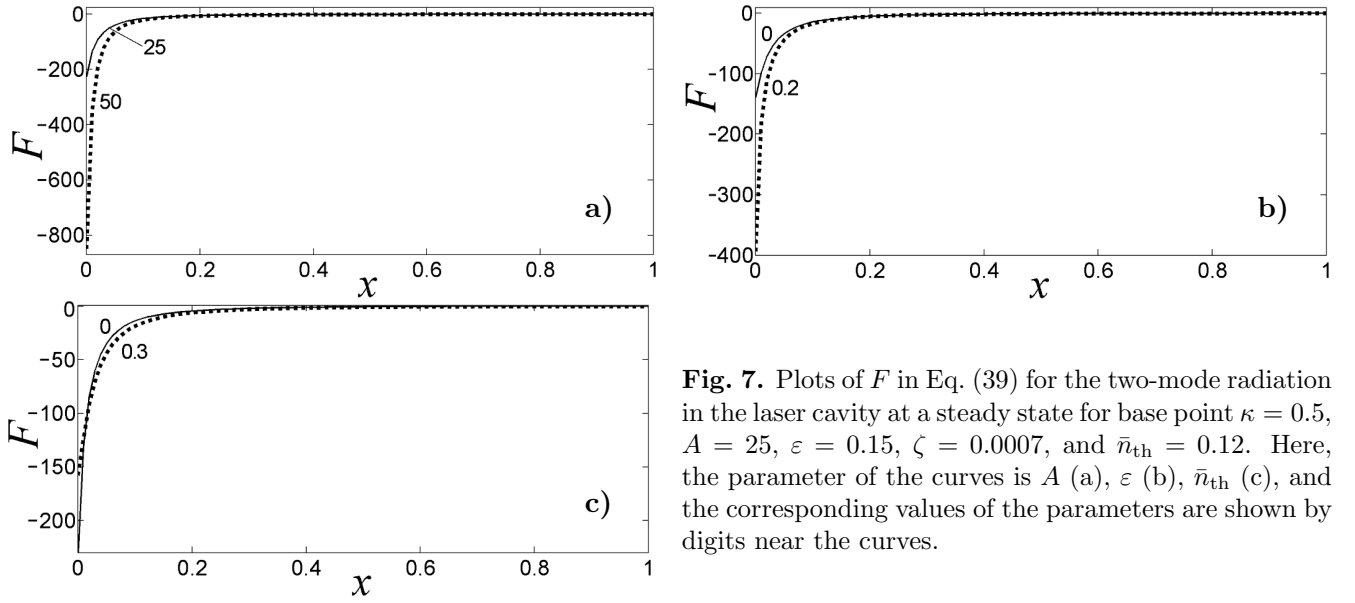


**Fig. 7.** Plots of  $F$  in Eq. (39) for the two-mode radiation in the laser cavity at a steady state for base point  $\kappa = 0.5$ ,  $A = 25$ ,  $\varepsilon = 0.15$ ,  $\zeta = 0.0007$ , and  $\bar{n}_{\text{th}} = 0.12$ . Here, the parameter of the curves is  $A$  (a),  $\varepsilon$  (b),  $\bar{n}_{\text{th}}$  (c), and the corresponding values of the parameters are shown by digits near the curves.

of atoms with equal probabilities at the upper and down levels.

### 3.4. Violation of Cauchy–Schwarz Inequality (CSI)

The other relevant criterion of entanglement for the two-mode light is the violation of the Cauchy–Schwarz inequality (CSI). This criterion is related to the second-order correlation function to determine the entanglement exhibited by the quantum system [34, 38]. Two-mode radiation in the laser cavity is said to be entangled if it violates the Cauchy–Schwarz inequality, which can be put in the form  $\langle \hat{a}^{\dagger 2} \hat{a}^2 \rangle \langle \hat{b}^{\dagger 2} \hat{b}^2 \rangle \geq \langle \hat{a}^{\dagger} \hat{a} \hat{b}^{\dagger} \hat{b} \rangle^2$ . The entanglement of the cavity radiation can be investigated by this criterion after normalization to the right-hand side of the inequality to obtain the correlation coefficient [38]

$$C_{\alpha\beta} = \frac{|\langle \hat{a}^{\dagger} \hat{a} \hat{b}^{\dagger} \hat{b} \rangle|}{\sqrt{\langle \hat{a}^{\dagger 2} \hat{a}^2 \rangle \langle \hat{b}^{\dagger 2} \hat{b}^2 \rangle}}, \quad (40)$$

in which the two-mode light is entangled when  $C_{\alpha\beta} \geq 1$  [34, 38].

Since the operators are already put in the normal order,  $C_{\alpha\beta}$  can be expressed in terms of the  $c$ -number zero mean Gaussian variables  $\alpha$  and  $\beta$  at a steady state as follows:

$$C_{\alpha\beta} = \frac{|\langle \alpha^* \alpha \beta^* \beta \rangle|}{\sqrt{\langle \alpha^{*2} \alpha^2 \rangle \langle \beta^{*2} \beta^2 \rangle}}, \quad (41)$$

where

$$\langle \alpha^* \alpha \beta^* \beta \rangle = \langle \alpha^* \alpha \rangle \langle \beta^* \beta \rangle + \langle \alpha \beta \rangle^2, \quad \langle \alpha^{*2} \alpha^2 \rangle = 2 \langle \alpha^* \alpha \rangle^2, \quad \langle \beta^{*2} \beta^2 \rangle = 2 \langle \beta^* \beta \rangle^2. \quad (42)$$

Now applying Eq. (42), we find that

$$C_{\alpha\beta} = \frac{1}{2} \left[ 1 + \frac{\langle \alpha \beta \rangle^2}{\langle \alpha^* \alpha \rangle \langle \beta^* \beta \rangle} \right]. \quad (43)$$

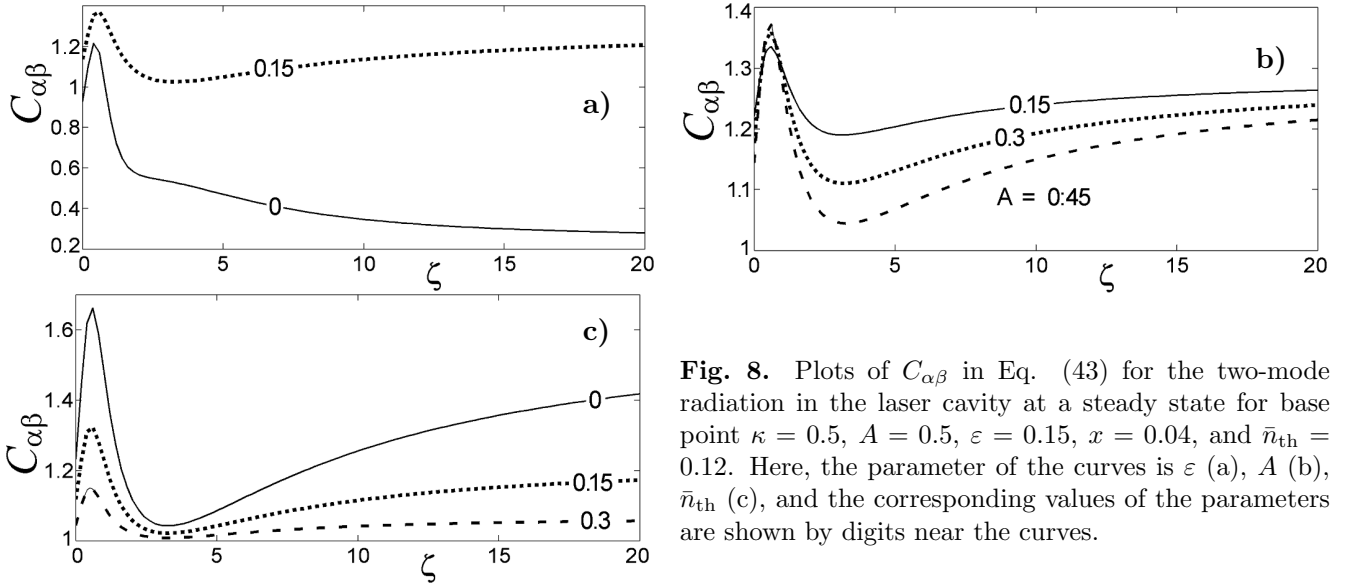


**Fig. 8.** Plots of  $C_{\alpha\beta}$  in Eq. (43) for the two-mode radiation in the laser cavity at a steady state for base point  $\kappa = 0.5$ ,  $A = 0.5$ ,  $\varepsilon = 0.15$ ,  $x = 0.04$ , and  $\bar{n}_{\text{th}} = 0.12$ . Here, the parameter of the curves is  $\varepsilon$  (a),  $A$  (b),  $\bar{n}_{\text{th}}$  (c), and the corresponding values of the parameters are shown by digits near the curves.

It can be verified with the help of [13, 27] that  $C_{\alpha\beta} = \frac{g^{(2)}(0)}{2}$ , in which  $g^{(2)}(0) = 1 + \frac{\langle\alpha\beta\rangle^2}{\langle\alpha^*\alpha\rangle\langle\beta^*\beta\rangle}$  is the equal-time second-order (intensity) correlation function. Hence we realize that the Cauchy–Schwarz inequality criterion can be also studied by the second-order correlation function. In addition, the radiation generated in the laser cavity would be categorized as bunched, antibunched, and coherent based on the value of the parameter  $C_{\alpha\beta}$ . Based on this, some authors call  $C_{\alpha\beta}$  a photon number correlation as it should be [13].

In order to investigate the entanglement of radiation in the laser cavity, we analyzed the variation of  $C_{\alpha\beta}$  with the  $\zeta$ ,  $\kappa$ ,  $\varepsilon$ ,  $x$ , and  $A$ . We also compare this approach with the other entanglement criteria.

It is clearly presented in Fig. 8 a that the CSI demonstrates the absence of entanglement for  $\varepsilon = 0$ , but the entanglement is detected at  $\zeta = 0.5$  (in the weak driving radiation regime). The same situation is also observed in the Hillary–Zubairy criterion. However, the radiation in the laser cavity is totally not entangled for  $\varepsilon = 0$  as predicted by the DGCZ and logarithmic negativity criteria. Also we immediately observe that the presence of the parametric amplifier leads to the violation of the Cauchy–Schwarz inequality showing that the radiation is now entangled. It is easy to observe that there is no any disparity among the criteria we considered in predicting the entanglement of radiation in the laser cavity for  $\varepsilon = 0.2$ . Furthermore, we present in Fig. 8 c the variation of the parameter  $C_{\alpha\beta}$  with  $A$  and  $\zeta$ . Hence, it is found that  $C_{\alpha\beta} \geq 1$  for all parameters under consideration. This is an indication of the fact that the cavity radiation is entangled. In addition, the dependence of the degree of entanglement on the linear gain coefficient is observed to be of a similar pattern as in Figs. 8 c and 4 c.

In contrast to the results presented in Fig. 8 a and b, we indicate in Fig. 8 c that  $C_{\alpha\beta}$  is found to decrease with increase in the mean photon number of the thermal reservoir. We found that the inequality condition completely restored for  $\bar{n}_{\text{th}} \geq 0.51$  indicating that the entanglement is destroyed.

We see in Fig. 8 that  $C_{\alpha\beta}$  becomes larger in the weak driving regime than in the strong driving one. Therefore, we seek to investigate the entanglement property of light in the laser cavity in the weak driving regime, where more improved degree of the entanglement can be produced by further manipulations of various parameters. Hence, we analyze the observed nonclassical property up on varying the amplitude



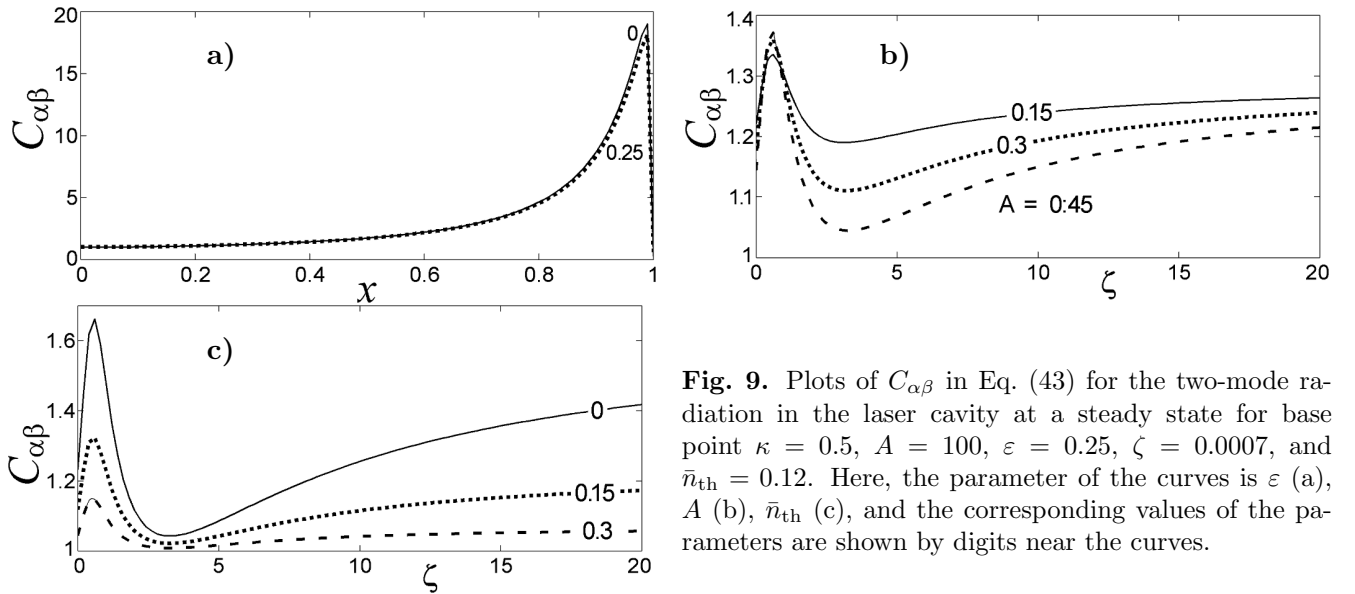


**Fig. 9.** Plots of  $C_{\alpha\beta}$  in Eq. (43) for the two-mode radiation in the laser cavity at a steady state for base point  $\kappa = 0.5$ ,  $A = 100$ ,  $\varepsilon = 0.25$ ,  $\zeta = 0.0007$ , and  $\bar{n}_{th} = 0.12$ . Here, the parameter of the curves is  $\varepsilon$  (a),  $A$  (b),  $\bar{n}_{th}$  (c), and the corresponding values of the parameters are shown by digits near the curves.

of the parametric amplifier, the linear gain coefficient, the mean photon number of thermal reservoir, and the initial preparation of the atoms in the regime.

We first investigate the variation of the minus quadrature variance with the injected atomic coherence and amplitude of the parametric amplifier fixing the rest parameters on the values that optimize the degree of entanglement. Also the increment of  $C_{\alpha\beta}$  up to  $x \simeq 0.97$  is related to the fact that the mean photon number of the separate cavity modes are smaller there.

In Fig. 9b, we see that the photon number correlation  $C_{\alpha\beta}$  decreases with the mean photon number of the thermal environment but increases by decreasing the injected atomic coherence. Thus, this criterion correctly demonstrates the influence of thermal noise on the entanglement of light in the laser cavity particularly at  $x = 1$ . In the absence of thermal noise,  $C_{\alpha\beta}$  grows significantly by decreasing the injected atomic coherence. Comparison of this criterion with the other three criteria in this particular case shows failure of the CSI criterion to correctly demonstrate the entanglement of light in the laser cavity. This situation is also consistent with the result reported in [13,27]. The introduction of the effect of thermal noise reverses such disparity particularly at  $x = 1$ , at which all the entanglement criteria indicate the absence of entanglement altogether.

## 4. Conclusions

In this work, we analyzed in detail the entanglement of the twin-beam generated by a coherent beat with a nondegenerate parametric amplifier and coupled to two-mode thermal reservoir, using the master equation approach. First, the master equation in the good-cavity limit with the linear and adiabatic approximations was determined. Applying the master equation, the time evolution of the first and second moments of the cavity mode variables were derived. With the help of these results, various quantities of interest were obtained.

The light generated by the quantum system exhibits entanglement for proper choices of the injected and driven atomic coherences. In particular, this nonclassical feature is strong in the weak and strong

classical field amplitudes and for the case where 48% probability of the atoms are initially prepared in the upper level. We showed that the entanglement quantification criteria studied by the logarithmic negativity and DGCZ criteria demonstrate the same pattern of entanglement although the former criterion has demonstrated 95.7% degree of entanglement, while the latter one has quantified 73.4% in the presence of thermal decoherence. On the other hand, the Hillary–Zubairy criterion and Cauchy–Schwarz inequality demonstrated the presence and variation of entanglement with the considered parameters exactly similar to the DGCZ and logarithmic negativity criteria. However, an issue that may arise regarding the Hillary–Zubairy criterion and the Cauchy–Schwarz inequality consists in the fact they have no lower or upper limits. As a result, we could not exactly know the degree of entanglement produced with these criteria, but we can clearly point out the stronger and weaker one separately. In particular, all the considered criteria demonstrated the amplification of entanglement with the help of the parametric amplifier and effective rate of atomic injection. In contrast, thermal noise has destructive effect on the entanglement of radiation in the laser cavity. Therefore, the equal time entanglement is very sensitive to thermal reservoir and can be lost by small effect of a noisy external environment.

In general, after detailed calculations and analysis we conclude that the proposed quantum system can be utilized as a source of entanglement, which has potential applications in different fields including modern physics, especially in quantum technologies and applications. The idea presented here is also good and may be useful for most users in various research fields, especially in quantum optics, the cavity QED, and quantum information. Moreover, the entanglement exhibited is quite robust and hence can be used in quantum information processing tasks.

## Acknowledgments

The authors would like to thank the Research and Postgraduate Coordination Office and College of Natural Sciences of Jimma University for their support and encouragement during this research work.

## References

1. Z. Zhao, Y. Chen, A. Zhang, et al., *Nature*, **430**, 54 (2004).
2. G. Burkard, *J. Phys. Condens. Matter*, **19**, 233202 (2007).
3. J. Hofmann, M. Krug, N. Ortegel, et al., *Science*, **337**, 72 (2012).
4. A. Einstein, B. Podolsky, and R. Rosen, *Phys. Rev.*, **47**, 777 (1935).
5. S. Bell, *J. Phys.*, **1**, 195 (1964).
6. K. Heshami, D. G. England, P. C. Humphreys, et al., *J. Mod. Opt.*, **63**, 2005 (2016).
7. C. H. Bennett and D. P. DiVincenzo, *Nature*, **404**, 247 (2000).
8. S. Barzanjeh, S. Pirandola, and C. Weedbrook, *Phys. Rev. A*, **88**, 042331 (2013).
9. J. G. Ren, P. Xu, H. L. Yong, et al., *Nature*, **549**, 70 (2017).
10. C. L. Degen, F. Reinhard, and P. Cappellaro, *Rev. Mod. Phys.*, **89**, 035002 (2017).
11. C. W. Gardiner, *Phys. Rev. Lett.*, **56**, 1917 (1986).
12. S. Qamar, S. Qamar, and M. S. Zubairy, *Opt. Commun.*, **283**, 781 (2010).
13. C. Gashu, E. Mosisa, and T. Abebe, *Adv. Math. Phys.*, **2020**, 14 (2020).
14. S. Tesfa, *Phys. Rev. A*, **79**, 063815 (2009).
15. N. A. Ansari, J. G. Banacloche, and M. S. Zubairy, *Phys. Rev. A*, **41**, 5179 (1990).
16. H. Xiong, M. O. Scully, and M. S. Zubairy, *Phys. Rev. Lett.*, **94**, 023601 (2005).
17. T. Abebe, N. Gemechu, C. Gashu, et al., *Int. J. Opt.*, **2020**, 11 (2020).
18. M. Kiffner, M. S. Zubairy, J. Evers, and C. H. Keitel, *Phys. Rev. A*, **75**, 033816 (2007).

19. C. Gashu and T. Abebe, *Phys. Scr.*, **95**, 075105 (2020).
20. S. Tesfa, *J. Phys. B: At. Mol. Opt. Phys.*, **40**, 2373 (2007).
21. A. C. Blockley and D. F. Walls, *Phys. Rev. A*, **43**, 5049 (1991).
22. T. Abebe and C. G. Feyisa, *Braz. J. Phys.*, **50**, 495 (2020).
23. F. Kassahun, *Fundamental of Quantum Optics*, Lulu, North Caroline (2008).
24. G. New, *Introduction to Nonlinear Optics*, Cambridge University Press, New York (2011).
25. T. Abebe, N. Gemechu, K. Shogile, et al., *Rom. J. Phys.*, **65**, 107 (2020).
26. E. Alebachew and K. Fesseha, *Opt. Commun.*, **265**, 314 (2006).
27. C. G. Feyisa, *Braz. J. Phys.*, **50**, 379 (2020).
28. W. H. Louisell, *Quantum Statistical Properties of Radiation*, Wiley, New York (1973).
29. L. Viola, E. Knill, and S. Lloyd, *Phys. Rev.*, **82**, 7417 (1999).
30. H. Jeong, J. Lee, and M. S. Kim, *Phys. Rev. A*, **61**, 052101 (2000).
31. C. G. Feyisa, T. Abebe, N. Gemechu, et al., *J. Russ. Laser. Res.*, **41**, 563 (2020).
32. C. Gashu, *Int. J. Opt.*, **2020**, 3823916 (2020).
33. L. M. Duan, G. Giedke, J. I. Cirac, and P. Zoller, *Phys. Rev. Lett.*, **84**, 2722 (2000).
34. A. Sumairi, S. N. Hazmin, and C. R. Ooi, *J. Mod. Opt.*, **60**, 589 (2013).
35. G. Adesso, A. Serafini, and F. Illuminati, *Phys. Rev. A*, **70**, 022318 (2004).
36. S. Tesfa, *Phys. Rev. A*, **74**, 043816 (2006).
37. M. Hillery and M. S. Zubairy, *Phys. Rev. Lett.*, **96**, 050503 (2006).
38. O. Jeff, *Quantum Optics for Experimentalists*, World Scientific, USA (2017).